

# Chaperone Peptides of $\alpha$ -Crystallin Inhibit Epithelial Cell Apoptosis, Protein Insolubilization, and Opacification in Experimental Cataracts<sup>\*[5]</sup>

Received for publication, November 28, 2012, and in revised form, March 6, 2013. Published, JBC Papers in Press, March 18, 2013, DOI 10.1074/jbc.M112.440214

Rooban B. Nahomi<sup>‡</sup>, Benlian Wang<sup>§</sup>, Cibin T. Raghavan<sup>‡</sup>, Oliver Voss<sup>¶</sup>, Andrea I. Doseff<sup>¶</sup>, Puttur Santhoshkumar<sup>¶</sup>, and Ram H. Nagaraj<sup>‡1</sup>

From the <sup>‡</sup>Department of Ophthalmology and Visual Sciences and <sup>§</sup>Center for Proteomics and Bioinformatics, Case Western Reserve University, Cleveland, Ohio 44106, the <sup>¶</sup>Davis Heart and Lung Research Institute, The Ohio State University, Columbus, Ohio 43210, and the <sup>¶</sup>Department of Ophthalmology, University of Missouri-Columbia, Columbia, Missouri 65212

**Background:** Peptides derived from the core domain of human  $\alpha$ -crystallin act as molecular chaperones.

**Results:** Chaperone peptides of  $\alpha$ -crystallin inhibit stress-induced apoptosis in cultured cells and prevent experimental cataracts in rats.

**Conclusion:** Chaperone peptides of  $\alpha$ -crystallin are anti-apoptotic and retain biological activity when injected into animals.

**Significance:**  $\alpha$ -Crystallin peptides could be used as therapeutic agents to inhibit protein aggregation and apoptosis in diseases.

$\alpha$ -Crystallin is a member of the small heat-shock protein (sHSP) family and consists of two subunits,  $\alpha$ A and  $\alpha$ B. Both  $\alpha$ A- and  $\alpha$ B-crystallin act as chaperones and anti-apoptotic proteins. Previous studies have identified the peptide <sup>70</sup>KFVIFLDVVKHFSPEDLTVK<sup>88</sup> in  $\alpha$ A-crystallin and the peptide <sup>73</sup>DRFSVNL DVKHFSP EELKVK<sup>92</sup> in  $\alpha$ B-crystallin as mini-chaperones. In the human lens, lysine 70 (Lys<sup>70</sup>) of  $\alpha$ A and Lys<sup>92</sup> of  $\alpha$ B (in the mini-chaperone sequences) are acetylated. In this study, we investigated the cellular effects of the unmodified and acetyl mini-chaperones. The  $\alpha$ A- and  $\alpha$ B-crystallin peptides inhibited stress-induced aggregation of four client proteins, and the  $\alpha$ A-acetyl peptide was more effective than the native peptide against three of the client proteins. Both the acetyl and native crystallin peptides inhibited stress-induced apoptosis in two mammalian cell types, and this property was directly related to the inhibition of cytochrome *c* release from mitochondria and the activity of caspase-3 and -9. In organ-cultured rat lenses, the peptides inhibited calcimycin-induced epithelial cell apoptosis. Intraperitoneal injection of the peptides inhibited cataract development in selenite-treated rats, which was accompanied by inhibition of oxidative stress, protein insolubilization, and caspase activity in the lens. These inhibitory effects were more pronounced for acetyl peptides than native peptides. A scrambled  $\alpha$ A-crystallin peptide produced no such effects. The results suggest that the  $\alpha$ -crystallin chaperone peptides could be used as therapeutic agents to treat cataracts and diseases in which protein aggregation and apoptosis are contributing factors.

$\alpha$ -Crystallin is the most abundant protein in the lens. It is composed of two subunits,  $\alpha$ A and  $\alpha$ B, whose sequences show significant homology to each other and to other small heat-shock proteins (1). The  $\alpha$ A- and  $\alpha$ B-crystallin heteropolymers are present in the lens as polydisperse oligomers with an average molecular mass of 800 kDa (2, 3).  $\alpha$ A-Crystallin is present mainly in the lens, whereas  $\alpha$ B-crystallin, in addition to the lens, is present in several other tissues, including the retina, heart, and kidney (4, 5). These peptides act as molecular chaperones and prevent the aggregation of structurally perturbed proteins. This chaperone function is thought to be essential in maintaining lens transparency during aging (6).

The anterior surface of the lens is covered with a single layer of cuboidal epithelial cells, which are important for maintaining metabolic homeostasis and lens transparency. Several studies have detected lens epithelial cell apoptosis in cataractous lenses (7, 8).  $\alpha$ -Crystallin acts as both a chaperone protein and anti-apoptotic protein; it inhibits apoptosis due to external stress in many cell types, including lens epithelial cells (9–14). The anti-apoptotic function of  $\alpha$ -crystallin is due to inhibition of procaspase-3 activation, binding to Bax, and prevention of its translocation to the mitochondria, inhibition of cytochrome *c* release from the mitochondria, activation of PI 3-kinase, and inhibition of PTEN (12, 15–17).  $\alpha$ -Crystallin has also been shown to mediate anti-inflammatory effects by binding to inflammatory cytokines (18, 19).

Protein turnover is negligible in the lens; thus proteins, including  $\alpha$ -crystallin, accumulate post-translational modifications. Major post-translational modifications include deamidation, truncation, glycation, and acetylation, which induce structural as well as functional changes and may contribute to cataract formation (20–23). In a previous study, we found that  $\alpha$ -crystallin is acetylated at discrete lysine residues in the human lens, and such acetylation improves its chaperone function (24). We identified acetylation sites at Lys<sup>70</sup> and Lys<sup>99</sup> in  $\alpha$ A-crystallin as well as Lys<sup>92</sup> and Lys<sup>166</sup> in  $\alpha$ B-crystallin.

\* This work was supported, in whole or in part, by National Institutes of Health Grants R01EY-022061 and R01EY-09912 (to R. H. N.), and P30EY-11373 to the Visual Sciences Research Center of Case Western Reserve University, and grants from the Research to Prevent Blindness, NY (to Case Western Reserve University and the University of Missouri-Columbia) and The Ohio Lions Eye Research Foundation.

[5] This article contains supplemental Figs. S1–S3.

<sup>1</sup> To whom correspondence should be addressed: Rm. 311, 2085 Adelbert Rd., Cleveland, OH 44106. Tel.: 216-368-2089; E-mail: ram.nagaraj@case.edu.

Previous studies have found short peptides within  $\alpha$ A- and  $\alpha$ B-crystallin that function as molecular chaperones, similar to the parent molecules. These peptides are  $^{70}$ KFVIFLDVKHFSPEDLTVK $^{88}$  in  $\alpha$ A-crystallin and  $^{73}$ DRFSVNLVDVKHFSPEELKVK $^{92}$  in  $\alpha$ B-crystallin (25, 26). Interestingly, two of the major acetylation sites in  $\alpha$ A- and  $\alpha$ B-crystallin (Lys $^{70}$  and Lys $^{92}$ , respectively) are located in these peptide sequences. Thus, we sought to determine the impact of lysine acetylation on the function of these peptides. In this study, we show that the  $\alpha$ -crystallin mini-chaperones and acetyl derivatives can inhibit apoptosis in mammalian cells by blocking cytochrome *c* release from mitochondria and preventing procaspase-3 activation. Using rats, we also present evidence that these peptides can inhibit protein aggregation and epithelial cell apoptosis in cataracts.

## EXPERIMENTAL PROCEDURES

Insulin, Hoechst, citrate synthase, sodium selenite, and a protease inhibitor mixture were obtained from Sigma. The remaining chemicals were of analytical grade.

$\alpha$ A-Crystallin peptides (native and acetyl:  $^{69}$ DKFVIFLDVKHFSPELTVK $^{88}$  and  $^{69}$ DK(acetyl)FVIFLDVKHFSPELTVK $^{88}$ ) and  $\alpha$ B-crystallin peptides (native and acetyl:  $^{73}$ DRFSVNLVDVKHFSPEELKVK $^{93}$  and  $^{73}$ DRFSVNLVDVKHFSPEELKVK(acetyl)V $^{93}$ ) as well as the scrambled peptide DFVIDSPFKLVLDLEKVVHFTK were synthesized, processed to 95–99% purity, and verified via mass spectrometry (for molecular weight and purity) by Peptide 2.0 (Chantilly, VA).

*Chaperone Assays*—Chaperone assays were performed as previously described (24). The ratios of the peptides:client proteins (w/w) were as follows: citrate synthase, 1:2.5; insulin, 1:10;  $\beta$ L-crystallin, 1:1.5; and  $\gamma$ -crystallin, 1:1. The scrambled  $\alpha$ A-crystallin peptide was tested in certain assays at peptide:client protein ratios as follows: citrate synthase, 1:1.25, and insulin, 1:5, to determine peptide specificity.

*Measurement of Peptide Surface Hydrophobicity*—The surface hydrophobicity of the peptides was measured using 6-(*p*-toluidinyl)naphthalene-2-sulfonic acid (emission, 350–520 nm; excitation, 320 nm) as previously described (24).

*Measurement of Apoptosis*—Human lens epithelial cells (HLE) $^2$  were isolated from the lens of a 44-year-old donor and cultured in DMEM supplemented with 10% FBS as previously described for mouse lens epithelial cells (27). Cells between passages 5 and 6 were used for the experiments. Chinese hamster ovary (CHO) cells were cultured in Ham's F-12 medium. The  $\alpha$ -crystallin peptides were mixed with a cationic lipid, BioPORTER $^{\text{®}}$ , according to the manufacturer's instructions (Polyplus transfection reagent, Illkirch, France). When the cultures reached 70–80% confluence, the cells were treated with BioPORTER either alone or with the peptides in serum-free medium and incubated for 4 h at 37 °C in a humidified 5% CO $_2$  atmosphere. The cells were then washed with PBS and incubated at 43 °C for 1 h (thermal stress), followed by incubation at 37 °C for 16 h for recovery. The percentage of apoptotic cells

was determined by staining the cells with Hoechst. Cells incubated at 37 °C without thermal stress were used as controls.

*Quantitation of Cytoplasmic Cytochrome *c**—Cell lysates were prepared in cell lysis buffer (Cell Signaling Technologies, Danvers, MA) with a protease inhibitor mixture (1:100 dilution). Western blotting was performed using 10  $\mu$ g of protein with a monoclonal antibody for cytochrome *c* (1:1,000 dilution, Enzo Life Sciences, Farmingdale, NY). The membrane was re-probed using an antibody for GAPDH (1:1,000 dilution, Millipore, Billerica, MA) as a loading control.

*Quantitation of Caspase-3 and Caspase-9 Activity*—Cells were lysed in cell lysis buffer (Cell Signaling), and lenses were homogenized in 50 mM Tris-buffered saline. Both buffers contained a protease inhibitor mixture (1:100 dilution). An equal volume of a fluorogenic substrate solution (2 $\times$  reaction buffer: 10 mM DTT and 50  $\mu$ M Ac-DEVD-AFC (*N*-acetyl-Asp-Glu-Val-Asp-7-amido-4-trifluoromethylcoumarin) (for caspase-3) or Ac-LEHD-AFC (*N*-acetyl-Leu-Glu-His-Asp-7-amido-4-trifluoromethylcoumarin) (for caspase-9)) was added to each lysate. The lysates were then incubated for 2 h at 37 °C in the dark. The samples were analyzed with a Spectramax 4 spectrofluorometer (HORIBA Scientific, Edison, NJ) at excitation/emission wavelengths 400/505 nm.

*Pro-caspase-3 Activation Assay*—CHO cells were lysed with lysis buffer (Cell Signaling) containing a protease inhibitor mixture, as previously described (28). The extracts were centrifuged for 10 min at 14,000  $\times$  *g*, boiled for 5 min at 100 °C, and analyzed by SDS-PAGE and immunoblotting using anti- $\beta$ -tubulin antibody (Santa Cruz, CA) or antibodies for inactive caspase-3 (9665S, clone 8G10) and active caspase-3 (9661S, clone Asp $^{175}$ ). These antibodies were purchased from Cell Signaling (12).

*Lens Organ Culture with Calcimycin*—The animal experiments conformed to the ARVO Statement for the Use of Animals in Ophthalmic and Vision Research and were approved by the Case Western Reserve University Animal Care and Use Committee. Lenses were dissected from the eyes of  $\sim$ 3-month-old C57Bl/6 mice and maintained in artificial aqueous humor (113 mM NaCl, 4.5 mM KCl, 1 mM MgCl $_2$ , 1.5 mM CaCl $_2$ , 6 mM D-glucose, 10 mM HEPES, 20 mM NaHCO $_3$ , and 1:1,000 penicillin/streptomycin, pH 7.3). Lenses that developed opacification within 24 h were discarded. Native and acetyl  $\alpha$ A- and  $\alpha$ B-crystallin peptides were added to the culture medium at a concentration of 50  $\mu$ g/3.0 ml, followed by incubation of the lenses for 16 h. The medium was replaced with fresh medium containing 5  $\mu$ M calcimycin, and the lenses were incubated for an additional 6 h. After this incubation period, the lenses were thoroughly washed with PBS, fixed in 1% buffered formalin overnight, and embedded in paraffin. Microtome sections (5  $\mu$ m) were subsequently rehydrated and subjected to antigen retrieval via microwave irradiation in 10 mM citrate buffer (pH 6.0). Apoptosis was measured using the *In situ* Cell Death Detection Kit (Roche Applied Science) according to the manufacturer's instructions. The sections were counterstained with DAPI to visualize nuclei.

*Selenite-induced Cataract and Apoptosis in Lens Epithelial Cells*—Neonatal Sprague-Dawley rat pups (12 days old) were used for these experiments. The pups in the experimental

$^2$  The abbreviations used are: HLE, human lens epithelial; SOD1, Cu/Zn-superoxide dismutase; MALS-DLS, multiangle light scattering/dynamic light scattering; CS, citrate synthase.

## Anti-apoptotic Properties of Crystallin Peptides

groups received a single subcutaneous injection of sodium selenite (4 mg/kg of body weight) on day 12. Peptides diluted from a stock in sterile water (dissolved by adding 2  $\mu$ l of 10 N NaOH to a 1.0-ml stock) were injected intraperitoneally (at 2.5, 5, or 10  $\mu$ g/animal) 6 h prior to selenite injection (single injection). When multiple injections were performed, one pre-selenite injection was administered, as above, followed by four additional injections on four consecutive days after the sodium selenite injection. One group served as the control (no treatment) and another as the selenite control (no peptide injection). The lenses were examined on day 18 (when the pups had opened their eyes) using a slit lamp microscope (after dilating the pupil through topical application of tropicamide) and photographed. For hematoxylin and eosin (H&E staining) and TUNEL staining, eyes were fixed immediately after enucleation in a 10% buffered formalin solution overnight.

**Quantitation of Water-soluble Proteins and  $\beta$ B1-Crystallin**—A subset of the lenses obtained from the above treatment groups was homogenized in ice-cold PBS containing 2  $\mu$ M Tris(2-carboxyethyl)phosphine hydrochloride (TCEP) and 5  $\mu$ l of a protease inhibitor mixture in a glass homogenizer (200  $\mu$ l for each lens). The homogenate was centrifuged at 20,000  $\times$  g for 30 min at 4  $^{\circ}$ C, and the supernatant was collected. The pellet was then homogenized again with the same buffer (100  $\mu$ l), centrifuged, and the supernatant collected. The two supernatant fractions were pooled, which was considered the water-soluble fraction. The pellet was considered the water-insoluble fraction. The latter fraction was solubilized in buffer with 6 M urea. The protein concentration was measured using the BCA Protein Assay Kit (Thermo Scientific, Rockford, IL), with BSA as the standard. SDS-PAGE was performed using 12% reducing gels to analyze the two fractions.  $\beta$ B1-Crystallin in the water-insoluble fraction (10  $\mu$ g of protein) was detected via Western blotting using a rabbit polyclonal antibody for  $\beta$ B1-crystallin from Santa Cruz Biotechnology (Santa Cruz, CA) (1:400 dilution) and a Chemiluminescence Detection Kit (Thermo Scientific).

**Markers of Oxidative Stress in Rat Lenses**—The concentration of GSH in the lens was determined as previously described (29), as was the SOD1 activity in the lens homogenates (30). Briefly, the assay mixture (total volume = 2.0 ml) contained sodium pyrophosphate buffer (52 mM, pH 8.3), 186  $\mu$ M phenazine methosulfate, 300  $\mu$ M nitro blue tetrazolium, and the homogenate (200  $\mu$ g). The reaction was initiated by adding 5.2 mM NADH (300  $\mu$ l) at a final concentration of 780  $\mu$ M, and the mixture was incubated at 30  $^{\circ}$ C for 1 min. The reaction was quenched by adding 1.0 ml of acetic acid, and the mixture was stirred vigorously. *n*-Butanol (5.0 ml) was next added to the mixture, followed by mixing and incubation at room temperature for 10 min. The mixture was finally centrifuged at 1,000  $\times$  g for 10 min, after which the butanol layer was separated, and the absorbance was measured at 560 nm against a butanol blank.

**Multiangle Light Scattering/Dynamic Light Scattering (MALS-DLS) Experiment**—Soluble lens proteins (190  $\mu$ g) were prepared as described above and injected into an HPLC/TSKPWxL5000 column with PBS as the eluent at 0.75

ml/min. The remaining details regarding MALS-DLS were reported previously (31). The data were analyzed using ASTRA software, developed by Wyatt Technologies (Santa Barbara, CA).

**Detection of Intraperitoneally Injected  $\alpha$ B-Crystallin Peptide in Rat Lenses**—Ten-day-old Sprague-Dawley rat pups ( $n = 6$ ) were intraperitoneally injected with 100  $\mu$ g of the acetyl  $\alpha$ B-crystallin peptide in 100  $\mu$ l of sterile water on four consecutive days. The control animals ( $n = 6$ ) were only injected with sterile water. The animals were sacrificed 3 h after the last injection, and their lenses were removed and homogenized in 500  $\mu$ l of PBS with 6 M urea. The homogenate was filtered through a 10-kDa cut-off centrifugal filter, and the filtrate was analyzed by LC-MS/MS using an Orbitrap Elite Hybrid Mass Spectrometer (Thermo Electron, San Jose, CA) equipped with the Waters nanoAcquity UPLC system (Waters, Taunton, MA). A full scan at 120,000 resolution was obtained in the Orbitrap spectrometer for the eluted peptides in the 300–1,800 atomic mass unit range, followed by 20 MS/MS scans; 17 of these were used to sequence the 17 most abundant precursor ions determined from the full scan, which were fragmented in the ion trap. The remaining 3 scan events employed an inclusion list to target the acetyl  $\alpha$ B-crystallin peptide  $^{73}$ DRESVNLVDVKHFSPEELKVK(acetyl)V $^{93}$  (632.84(4+), 843.45(3+), and 1264.68(2+)). MS/MS spectra were generated through collision-induced dissociation of the peptide ions at a 35% normalized collision energy to produce a series of *b*- and *y*-ions as major fragments using dynamic exclusion with a repeat count of 2, repeat duration of 30 s, exclusion duration of 30 s, and exclusion size list of 500. The total analysis time was 90 min. Raw LC-MS/MS data were subjected to database searches using the Mascot search engine (version 2.2.0, Matrix Science) against the human SwissProt database (20,249 sequences) with the variable modifications of Met oxidation and Lys acetylation and the enzyme cleavage set to none. The mass tolerance was set at 10 ppm for precursor ions and 0.8 Da for product ions. The significance threshold was  $p < 0.05$ .

**Statistical Analysis**—The data are presented as the mean  $\pm$  S.D. from the experiment numbers indicated in the figure legends. The data were analyzed using StatView software (SAS Institute Inc., Cary, NC). The statistical significance was evaluated with a paired or unpaired two-tailed *t* test, and differences were considered significant at  $p < 0.05$ .

## RESULTS

**$\alpha$ A- and  $\alpha$ B-Crystallin Peptides Inhibit Chemical and Thermal Protein Aggregation**—The chaperone function of the  $\alpha$ A- and  $\alpha$ B-crystallin peptides was evaluated using four client proteins, citrate synthase (CS), insulin,  $\beta$ L-crystallin, and  $\gamma$ -crystallin. The chaperone function of the acetyl  $\alpha$ A-crystallin peptide was significantly better than that of the native peptide for three of the client proteins. When  $\beta$ L-crystallin was used as the client protein, the results for two peptides were not different (Fig. 1A). In contrast, the acetyl  $\alpha$ B-peptide was 10–30% weaker than the native peptide for the above four client proteins (Fig. 1B). However, this change in the chaperone function observed for the acetyl peptides did not correspond to surface hydrophobicity; we observed no significant differ-

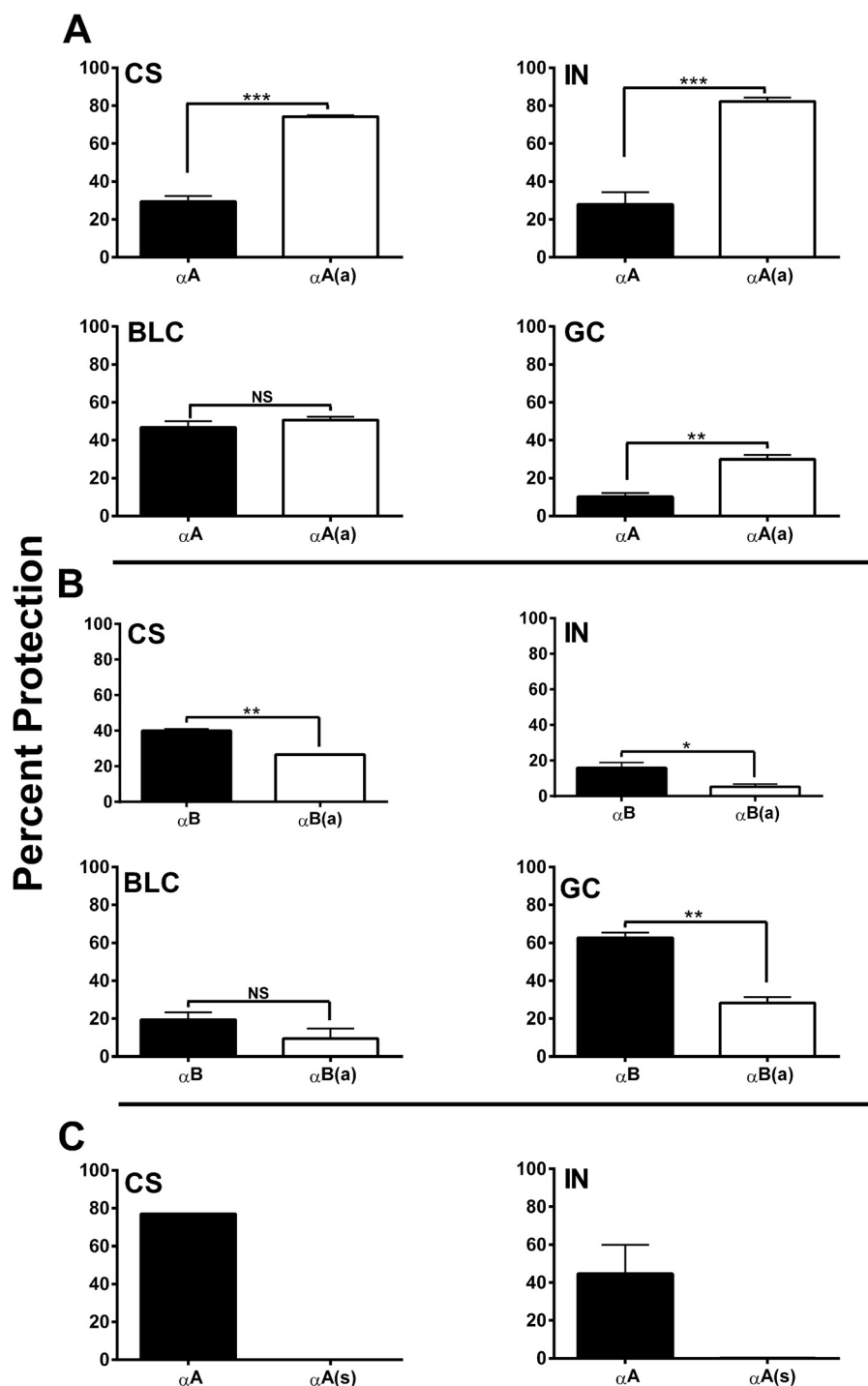


FIGURE 1. **Lysine acetylation differentially alters chaperone function in  $\alpha$ -crystallin peptides.** Native and acetyl  $\alpha A$ - and  $\alpha B$ -crystallin peptides were assessed for their chaperone function using four client proteins: citrate synthase (CS), insulin (IN),  $\beta_L$ -crystallin (BLC), and  $\gamma$ -crystallin (GC). The ratios of the client proteins to the peptides are given under "Experimental Procedures" except for the scrambled peptide, which was tested at a two times higher concentration. *Panel A* shows results for the  $\alpha A$  native ( $\alpha A$ ) and acetyl peptide ( $\alpha A(a)$ ), and *panel B* shows results for the  $\alpha B$  native ( $\alpha B$ ) and acetyl peptide ( $\alpha B(a)$ ). We also tested the scrambled  $\alpha A$ -crystallin peptide ( $\alpha A(s)$ ) with two client proteins, CS (peptide: CS-1:1.25) and insulin (peptide: IN-1:5); the results are shown in *panel C*. The bars represent the mean  $\pm$  S.D. of three independent assays. \*,  $p < 0.05$ ; \*\*,  $p < 0.005$ ; \*\*\*,  $p < 0.0005$ . NS, not significant.

ence in surface hydrophobicity between the acetyl and native peptides (supplemental Fig. S1). To test whether the chaperone function was dependent on the specific amino acid sequence of the peptides, we used a scrambled  $\alpha A$ -crystallin peptide in the chaperone assays. Our results showed that the scrambled peptide did not function as a chaperone for the two client proteins tested (CS and insulin), even when tested

at two times higher concentration than the native and acetyl peptides (Fig. 1C). The results confirmed that the specific peptide amino acid sequence in the peptide is a rigid requirement for chaperone function.

*$\alpha A$ - and  $\alpha B$ -Crystallin Peptides Inhibit the Mitochondrial Apoptosis Pathway in Thermally Stressed Cells*—We investigated the anti-apoptotic function of the native and acetyl  $\alpha A$ -

## Anti-apoptotic Properties of Crystallin Peptides

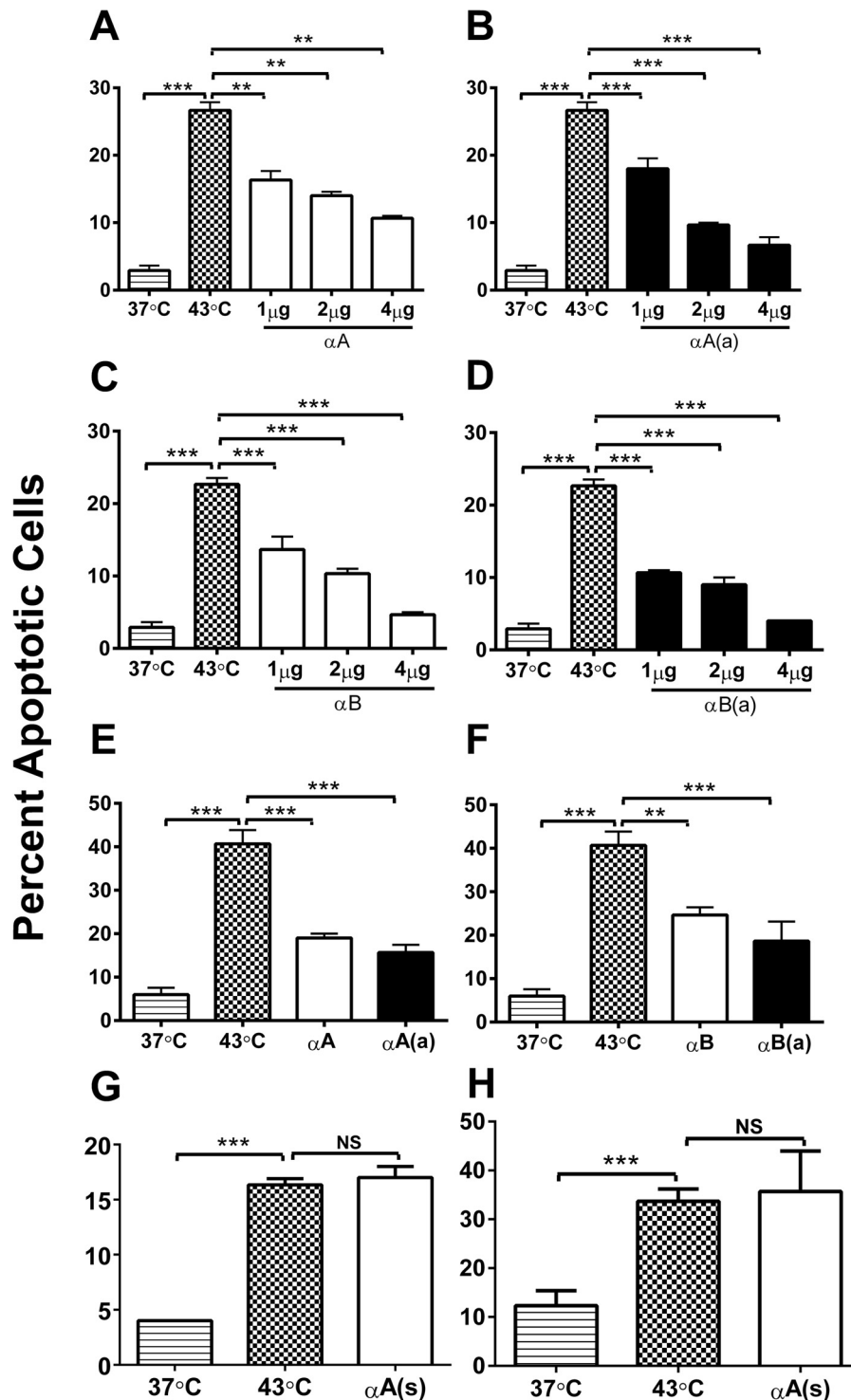


**FIGURE 2. Crystallin peptides are anti-apoptotic.** CHO cells were treated with native (panels A and C) or acetyl peptides (panels B and D) in BioPORTER at 1, 2, and 4  $\mu\text{g/ml}$  of medium for 4 h and subjected to thermal stress (43  $^{\circ}\text{C}$  for 1 h) to induce apoptosis. The anti-apoptotic function of the  $\alpha\text{A}$ -crystallin (panel E) and  $\alpha\text{B}$ -crystallin (panel F) peptides was also assessed in HLE cells. HLE cells were incubated with BioPORTER-treated peptides at 4  $\mu\text{g/ml}$  for 4 h and then at 43  $^{\circ}\text{C}$  for 1 h. CHO (panel G) and HLE cells (panel H) were treated with an  $\alpha\text{A}$ -scrambled peptide at 4  $\mu\text{g/ml}$  to determine peptide specificity. Apoptotic cells were counted after treating the cells with Hoechst stain. The bars represent the mean  $\pm$  S.D. of three independent experiments.  $\alpha\text{A}$ ,  $\alpha\text{A}$ -native peptide;  $\alpha\text{A(a)}$ ,  $\alpha\text{A}$ -acetyl peptide;  $\alpha\text{B}$ ,  $\alpha\text{B}$ -native peptide;  $\alpha\text{B(a)}$ ,  $\alpha\text{B}$ -acetyl peptide; and  $\alpha\text{A(s)}$ ,  $\alpha\text{A}$ -scrambled peptide. \*\*,  $p < 0.005$ ; \*\*\*,  $p < 0.0005$ . NS, not significant.

and  $\alpha\text{B}$ -crystallin peptides in CHO and HLE cells. The peptides were transferred to the cells using BioPORTER, and the cells were stressed at 43  $^{\circ}\text{C}$  for 1 h to induce apoptosis. The rate of hyperthermia-induced apoptosis was  $\sim 28\%$  in CHO cells (Fig.

2). Treatment with 1, 2, or 4  $\mu\text{g}$  of the  $\alpha\text{A}$ -crystallin peptide resulted in significant inhibition of apoptosis (by 12, 14, or 17%) ( $p < 0.005$  for each); the acetyl counterpart was at least 5% more effective than the native peptide at 2 and 4  $\mu\text{g}$  concentrations

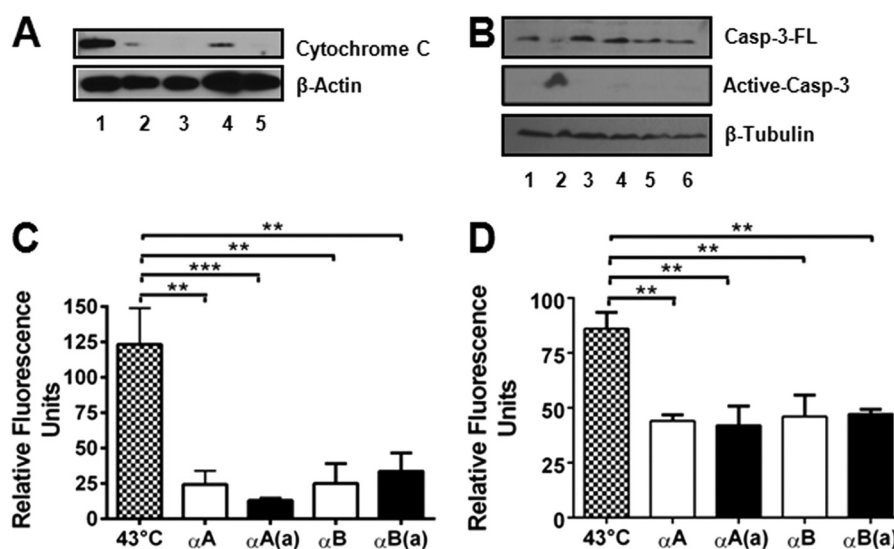


**FIGURE 3. The inhibition of hyperthermia-induced apoptosis by crystallin peptides occurs through blockade of the mitochondrial death pathway.** CHO cells were treated with peptides and thermally stressed, as described in the legend to Fig. 2.  $\alpha$ -Crystallin peptides inhibit cytochrome *c* release from the mitochondria (A). Cytochrome *c* release from the mitochondria into the cytosol was assessed via Western blotting. All lanes correspond to thermally stressed cells. Lane 1, no peptide; lane 2, + $\alpha$ A-native peptide; lane 3, + $\alpha$ A-acetyl peptide; lane 4, + $\alpha$ B peptide; and lane 5, + $\alpha$ B-acetyl peptide. Activation of procaspase-3 was inhibited by both acetyl and native peptides (B). *Casp-3-FL*, full-length procaspase-3; *Active-casp-3*, active caspase-3. Lane 1, control; lanes 2–6, thermally stressed cells; lane 2, no peptide; lane 3, + $\alpha$ A-native peptide; lane 4, + $\alpha$ A-acetyl peptide; lane 5, + $\alpha$ B peptide; and lane 6, + $\alpha$ B-acetyl peptide. Caspase-3 (C) and caspase-9 (D) activity was measured using specific fluorogenic substrates. Both  $\alpha$ A-crystallin and  $\alpha$ B-crystallin peptides inhibited caspase activity. The bars represent the mean  $\pm$  S.D. of three independent experiments.  $\alpha$ A,  $\alpha$ A-native peptide;  $\alpha$ A(a),  $\alpha$ A-acetyl peptide;  $\alpha$ B,  $\alpha$ B-native peptide; and  $\alpha$ B(a),  $\alpha$ B-acetyl peptide. The differences between the native and acetyl peptides were not statistically significant. \*\*,  $p < 0.005$ ; \*\*\*,  $p < 0.0005$ .

(Fig. 2, A and B). Similarly, the  $\alpha$ B-crystallin peptide inhibited apoptosis by 8, 12, and 17% at concentrations of 1, 2, and 4  $\mu$ g/ml, and the acetyl counterpart was 2–4% more effective than the native peptide at these concentrations (Fig. 2, C and D). To determine whether the anti-apoptotic function observed in CHO cells is relevant to lens epithelial cells, primary HLE cells were treated with the peptides in 4  $\mu$ g/ml of BioPORTER for 4 h and held at 43 °C for 1 h. At 37 °C, the cells did not undergo appreciable apoptosis. In contrast, cells at 43 °C exhibited significant apoptosis, at a rate of nearly 40% (Fig. 2E,  $p < 0.0005$ ). Pre-treatment with the native and acetyl  $\alpha$ A-crystallin peptides reduced the rates of apoptosis to 22 and 25%, respectively (Fig. 2E), whereas treatment with the native and acetyl  $\alpha$ B-crystallin peptides reduced the rates to 18 and 24%, respectively (Fig. 2F). These results indicate that the acetyl peptides are more effective than the native peptides in inhibiting apoptosis. The scrambled peptide did not inhibit apoptosis in either the CHO or HLE cells (Fig. 2, G and H).

The anti-apoptotic function of the peptides primarily occurred through inhibition of the mitochondrial apoptosis pathway, which was evident from the following observations. 1) The peptides inhibited the cytosolic release of cytochrome *c* from the mitochondria in thermally stressed CHO cells (Fig. 3A); the inhibition was greater for the acetyl peptides compared with the native peptides. 2) The peptides inhibited procaspase-3 maturation in thermally stressed CHO cells (Fig. 3B). Activated caspase-3 was detected only in cells that were not treated with the peptides. 3) The peptides significantly inhibited caspase-3 and -9 activity (Fig. 3, C and D). For these assays, we used peptides at a concentration of 4  $\mu$ g/ml. At this concentration, the  $\alpha$ A-peptide and its acetyl counter-

part inhibited caspase-3 activity by 80 and 90% and caspase-9 activity by 51 and 53%, respectively. At similar concentrations,  $\alpha$ B- and its acetyl counterpart inhibited caspase-3 activity by 80 and 78% and caspase-9 activity by 51 and 50%, respectively. These data show that both  $\alpha$ A- and  $\alpha$ B-crystallin peptides inhibit the mitochondrial apoptosis pathway in thermally stressed cells.

*$\alpha$ A- and  $\alpha$ B-Crystallin Peptides Inhibit Calcimycin-induced Apoptosis by Inhibiting Caspases in Organ-cultured Lenses*—To determine whether the peptides are effective at inhibiting apoptosis in whole lenses, we used organ-cultured mouse lenses. The lenses were incubated with calcimycin to induce apoptosis, as previously reported (32). Incubation with calcimycin induced apoptosis of epithelial cells, as observed by TUNEL staining (Fig. 4A, panel 2). Lenses not treated with calcimycin did not show apoptosis (Fig. 4A, panel 1). Prior treatment with the peptides (native or acetyl) inhibited calcimycin-induced epithelial cell apoptosis (Fig. 4A, panels 3 to 6). Quantitation of the numbers of TUNEL-positive cells revealed that  $\sim$ 33% of lens epithelial cells were apoptotic in calcimycin-treated lenses (Fig. 4B). Both the native and acetyl  $\alpha$ A- and  $\alpha$ B-crystallin peptides significantly inhibited apoptosis ( $p < 0.0005$ ), resulting in a rate of apoptosis of 3–5%. The scrambled peptide did not protect the cells (Fig. 4, A, panel 7, and B).

Apoptosis was inhibited through the mitochondrial apoptosis pathway, which was evident from the inhibition of caspase-3 and caspase-9 activity by both native and acetyl peptides (Fig. 4, C and D). These data suggest that both native and acetyl peptides can enter the lens epithelium through the capsule and inhibit mitochondrial-mediated apoptosis.

## Anti-apoptotic Properties of Crystallin Peptides

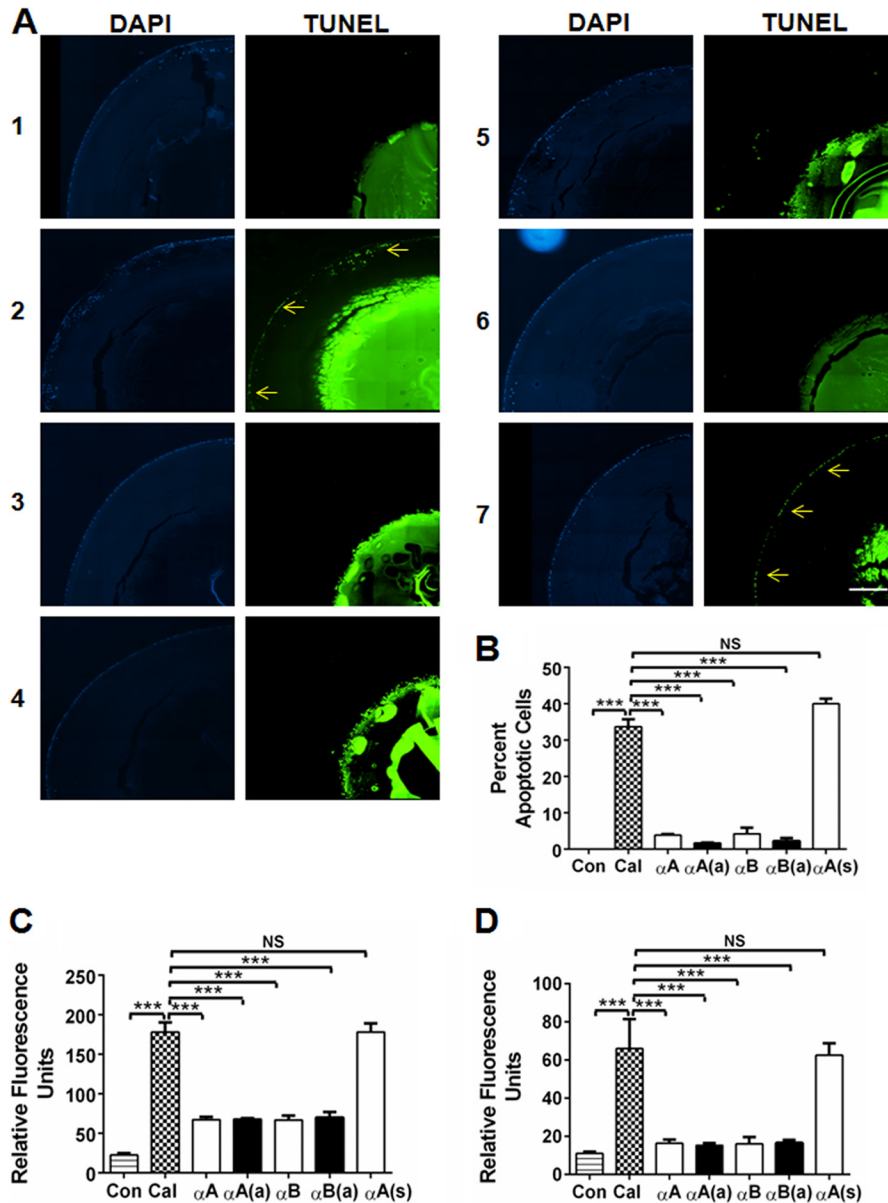


**FIGURE 4.  $\alpha$ -Crystallin peptides inhibit calcimycin-induced apoptosis in cultured mouse lenses.** Mouse lenses were organ cultured and treated with peptides, as described under "Experimental Procedures." After treatment, the lenses were thoroughly rinsed in PBS, fixed, and sectioned. The sections were stained to detect apoptotic cells using an *in situ* Apoptosis Detection Kit (A). *Left panels*, DAPI staining to visualize the nuclei in the lens epithelium; *right panels*, TUNEL staining to show apoptosis (arrows). *Panel 1*, control; *panels 2–7*, calcimycin-treated lenses. *Panel 2*, no peptide; *panel 3*, +  $\alpha A$ -native peptide; *panel 4*, +  $\alpha A$ -acetyl peptide; *panel 5*, +  $\alpha B$  peptide; *panel 6*, +  $\alpha B$ -acetyl peptide; and *panel 7*, scrambled  $\alpha A$ -peptide. The percentages of apoptotic cells are presented in a bar graph format in *panel B*. After culturing, the lenses were homogenized, and caspase-3 (C) as well as caspase-9 (D) activity was determined as described in the legend to Fig. 3. The bars represent the mean  $\pm$  S.D. of three independent experiments.  $\alpha A$ ,  $\alpha A$ -native peptide;  $\alpha A(a)$ ,  $\alpha A$ -acetyl peptide;  $\alpha B$ ,  $\alpha B$ -native peptide;  $\alpha B(a)$ ,  $\alpha B$ -acetyl peptide; and  $\alpha A(s)$ ,  $\alpha A$ -scrambled peptide. The differences between the native and acetyl peptides were not statistically significant. The intense TUNEL staining in the nuclear region is likely due to fragmented DNA in the terminally differentiated fiber cells. \*\*\*,  $p < 0.0005$ . NS, not significant. Scale bar = 100  $\mu$ m.

**$\alpha A$ - and  $\alpha B$ -Crystallin Peptides Inhibit Selenite-induced Cataracts in Rats**—Because the peptides inhibited lens epithelial cell apoptosis in organ-cultured lenses, we next tested whether they could inhibit cataract development in an experimental animal model. Cataracts were induced by injecting sodium selenite into 12-day-old rat pups. We injected the peptides either using a single intraperitoneal injection 6 h prior to sodium selenite injection or through multiple injections. In the case of multiple injections, the first injection was given 6 h prior to sodium selenite injection, followed by subsequent injections each day for 4 days. Mature cataracts were evident when the

sodium selenite-treated pups opened their eyes (Fig. 5, *top right panels*). When administered in a single 2.5- $\mu$ g injection, both the native and acetyl  $\alpha A$ -peptides were ineffective. At 5 and 10  $\mu$ g doses, the acetyl peptide was more effective than the native peptide in inhibiting cataract development. When administered as multiple 2.5- $\mu$ g injections, the acetyl peptide partially inhibited cataract development. At 5  $\mu$ g, both peptides strongly inhibited cataracts, and at 10  $\mu$ g, they entirely inhibited cataracts.

We also tested the native and acetyl  $\alpha B$ -crystallin peptides for selenite-cataract inhibition. Under the single injection reg-

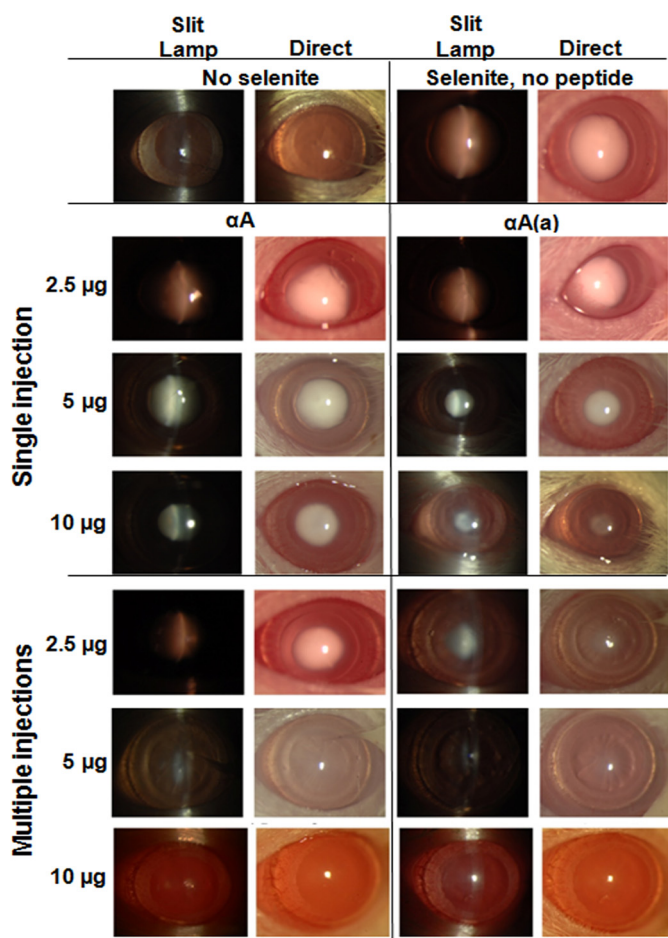


**FIGURE 5.  $\alpha$ A-Crystallin peptides inhibit cataracts in rats.** Sodium selenite was administered to 12-day-old rat pups to induce cataracts, as described under "Experimental Procedures." When single injections were used, native and acetyl  $\alpha$ A-crystallin peptides were intraperitoneally injected at 2.5, 5, and 10  $\mu$ g/animal 6 h prior to sodium selenite injection. When multiple injections were used, the peptides at the above doses were injected 6 h prior to and on days 1, 2, 3, and 4 days following sodium selenite injection. On day 6-post sodium selenite injection (when the pups were 18 days old and had opened their eyes), cataract formation was assessed via slit-lamp (left panels) and direct imaging (right panels). The control rats exhibited no cataracts (top left), whereas the sodium selenite-injected rats had mature cataracts (top right). The peptides inhibited cataract development; the acetyl peptide (single 5 and 10  $\mu$ g injections and multiple 2.5  $\mu$ g injections) was better than the native peptide at inhibiting cataract development. When multiple 10- $\mu$ g injections were administered, both peptides prevented cataract development. For each treatment group,  $n = 3$ . The data shown are from one representative animal/group.  $\alpha$ A,  $\alpha$ A-native peptide;  $\alpha$ A(a),  $\alpha$ A-acetyl peptide.

When multiple injections were used, the peptides at the above doses were injected 6 h prior to and on days 1, 2, 3, and 4 days following sodium selenite injection. On day 6-post sodium selenite injection (when the pups were 18 days old and had opened their eyes), cataract formation was assessed via slit-lamp (left panels) and direct imaging (right panels). The control rats exhibited no cataracts (top left), whereas the sodium selenite-injected rats had mature cataracts (top right). The peptides inhibited cataract development; the acetyl peptide (single 5 and 10  $\mu$ g injections and multiple 2.5  $\mu$ g injections) was better than the native peptide at inhibiting cataract development. When multiple 10- $\mu$ g injections were administered, both peptides prevented cataract development. For each treatment group,  $n = 3$ . The data shown are from one representative animal/group.  $\alpha$ A,  $\alpha$ A-native peptide;  $\alpha$ A(a),  $\alpha$ A-acetyl peptide.

When multiple injections were used, the peptides at the above doses were injected 6 h prior to and on days 1, 2, 3, and 4 days following sodium selenite injection. On day 6-post sodium selenite injection (when the pups were 18 days old and had opened their eyes), cataract formation was assessed via slit-lamp (left panels) and direct imaging (right panels). The control rats exhibited no cataracts (top left), whereas the sodium selenite-injected rats had mature cataracts (top right). The peptides inhibited cataract development; the acetyl peptide (single 5 and 10  $\mu$ g injections and multiple 2.5  $\mu$ g injections) was better than the native peptide at inhibiting cataract development. When multiple 10- $\mu$ g injections were administered, both peptides prevented cataract development. For each treatment group,  $n = 3$ . The data shown are from one representative animal/group.  $\alpha$ A,  $\alpha$ A-native peptide;  $\alpha$ A(a),  $\alpha$ A-acetyl peptide.

When multiple injections were used, the peptides at the above doses were injected 6 h prior to and on days 1, 2, 3, and 4 days following sodium selenite injection. On day 6-post sodium selenite injection (when the pups were 18 days old and had opened their eyes), cataract formation was assessed via slit-lamp (left panels) and direct imaging (right panels). The control rats exhibited no cataracts (top left), whereas the sodium selenite-injected rats had mature cataracts (top right). The peptides inhibited cataract development; the acetyl peptide (single 5 and 10  $\mu$ g injections and multiple 2.5  $\mu$ g injections) was better than the native peptide at inhibiting cataract development. When multiple 10- $\mu$ g injections were administered, both peptides prevented cataract development. For each treatment group,  $n = 3$ . The data shown are from one representative animal/group.  $\alpha$ A,  $\alpha$ A-native peptide;  $\alpha$ A(a),  $\alpha$ A-acetyl peptide.

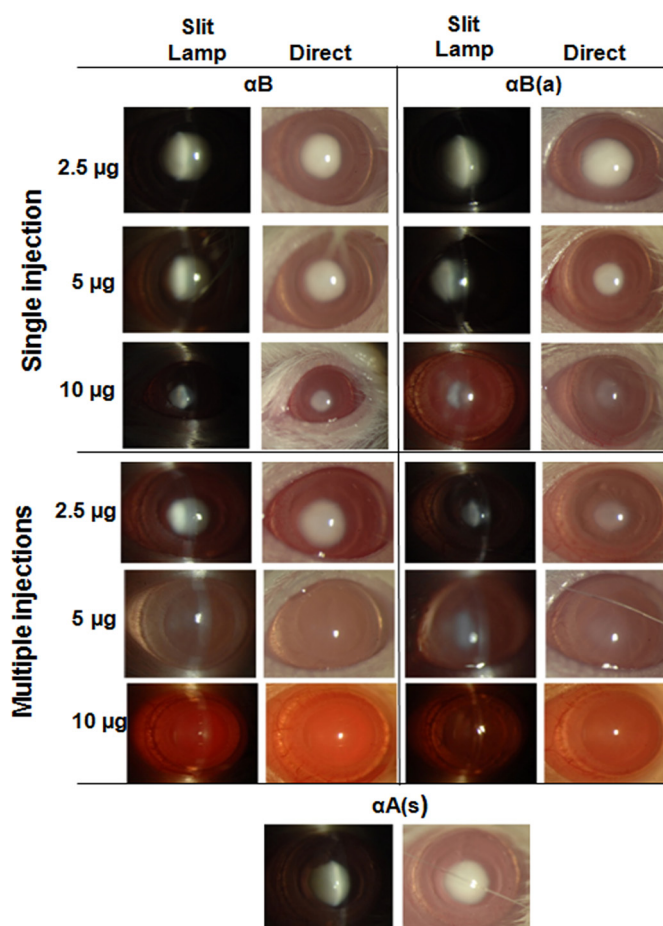


**FIGURE 6.  $\alpha$ B-Crystallin peptides inhibit cataracts in rats.** The experimental details are identical to those given in Fig. 5, except that the animals were injected with either the  $\alpha$ B-native peptide or  $\alpha$ B-acetyl peptide. The bottom panels show the results from rats treated with multiple injections (10  $\mu$ g/animal) of the scrambled  $\alpha$ A-crystallin peptide. The native and acetyl  $\alpha$ B-crystallin peptides exhibited a similar potency in inhibiting selenite-induced cataracts. In each treatment group,  $n = 3$ . The data shown are from one representative animal/group. Mild inhibition of cataract was evident following treatment with 5  $\mu$ g of the acetyl peptide, but not the native peptide. Following multiple injections at 10  $\mu$ g, both peptides inhibited cataract development.  $\alpha$ B,  $\alpha$ B-native peptide;  $\alpha$ B(a),  $\alpha$ B-acetyl peptide; and  $\alpha$ A(s),  $\alpha$ A-scrambled peptide. The scrambled peptide was ineffective in inhibiting cataract.

A histological examination of the selenite-treated cataract lenses showed protein aggregates in the nuclear region (supplemental Fig. S2). Peptide treatment corrected this change to control levels. Extraction of lenses in buffer, followed by protein quantity estimation, revealed a significant ( $p < 0.0005$ ; more than 50%) reduction of soluble protein associated with the selenite-induced cataracts (Fig. 7A). This reduction was significantly inhibited (70–80%) by both the native and acetyl peptides. Analyses of the water-soluble protein fraction via MALS-DLS revealed no covalent protein aggregation in the selenite-induced cataracts, and peptide treatment did not have an apparent effect on the protein profile (Fig. 7B). This was further confirmed via SDS-PAGE, which showed similar protein profiles for the water-soluble and insoluble fractions (Fig. 7, C and D). In selenite-induced cataracts in rats, m-calpain or calpain II were activated, which cleaves crystallins ( $\beta$ B1-crystallin in particular) (33). To determine whether the peptides inhibited such cleavage, we subjected the water-insoluble fraction to Western

## Anti-apoptotic Properties of Crystallin Peptides

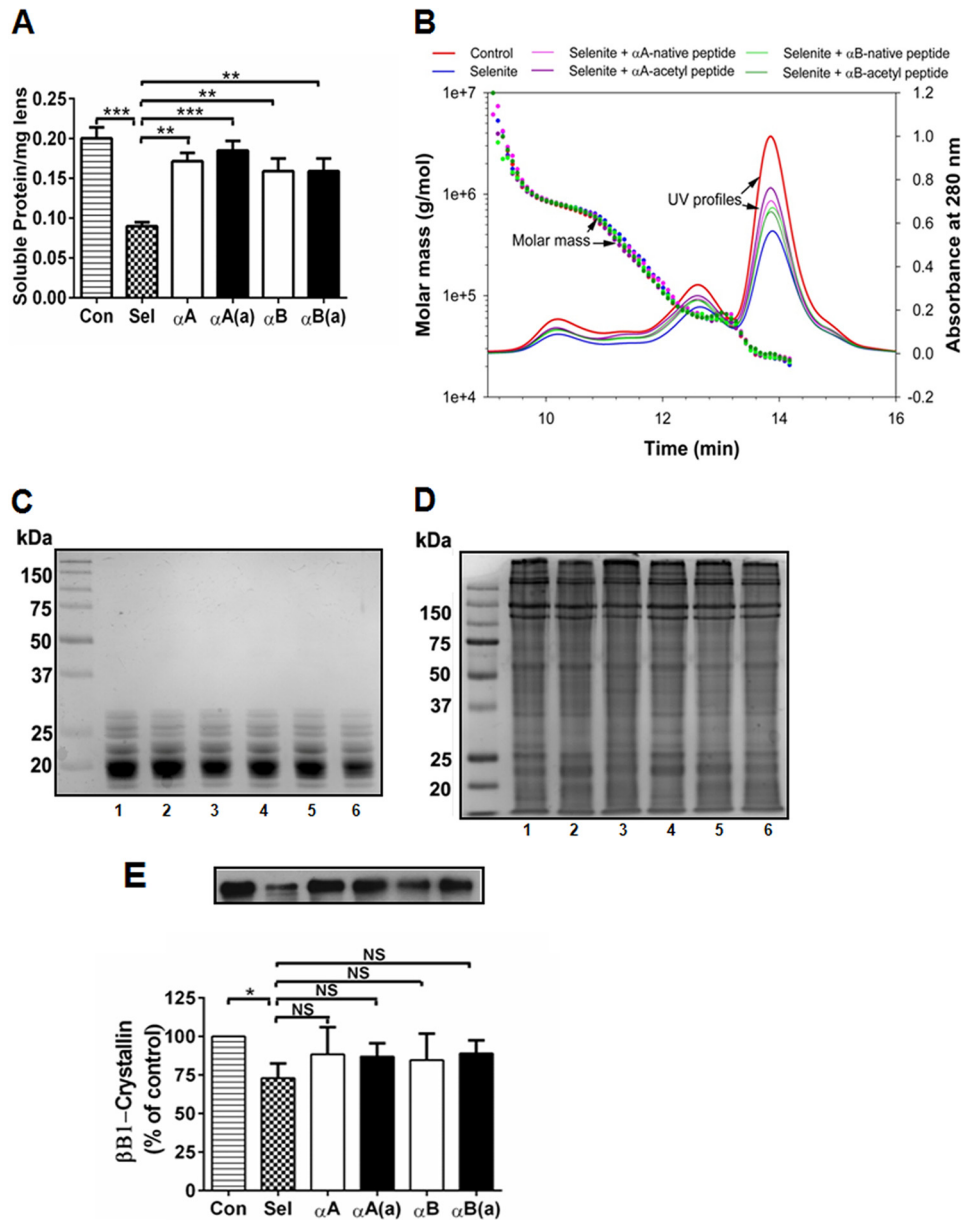


**FIGURE 7. In rats,  $\alpha$ -crystallin peptides inhibit protein insolubilization in selenite cataracts.** Cataracts were induced using sodium selenite, and the animals were treated with multiple 10- $\mu$ g peptide injections, as described in the legend to Fig. 5. The lenses were harvested from animals on day 6-post sodium selenite injection and processed as described under "Experimental Procedures." The water-soluble protein content decreased in the selenite-induced cataracts, which was significantly corrected by the native and acetyl peptides (panel A). MALS-DLS analyses of the water-soluble protein fraction from control, selenite-treated, and selenite + peptide-treated animals showed no apparent differences between groups (panel B). Water-soluble and insoluble proteins were analyzed by SDS-PAGE, which showed no additional protein cross-linking under either selenite or selenite + peptide treatment (panels C and D). 1, control; lanes 2–6, sodium selenite treated; 2, no peptide; 3, + $\alpha A$ -native peptide; 4, + $\alpha A$ -acetyl peptide; 5, + $\alpha B$  peptide; and 6, + $\alpha B$ -acetyl peptide. The cleavage of  $\beta B1$ -crystallin in the water-insoluble selenite cataract fraction (determined by Western blotting) was inhibited by peptide administration (panel E). The bars represent the mean  $\pm$  S.D. of three independent experiments. The differences between the native and acetyl peptides were not statistically significant. \*,  $p < 0.05$ ; \*\*,  $p < 0.005$ ; \*\*\*,  $p < 0.0005$ . NS, not significant.

blotting using a  $\beta B1$ -crystallin antibody. The results showed that  $\beta B1$ -crystallin was significantly reduced in selenite-induced cataracts ( $p < 0.05$ ), and both the acetyl and native crystallin peptides inhibited this reduction, although the effect was not significant (Fig. 7E).

Biochemical analyses of the lenses showed that the levels of GSH and the antioxidant enzyme SOD1 were significantly reduced in selenite-induced cataracts, which was mostly corrected by peptide administration (significantly for GSH; Fig.

8, A and B). This corrective effect was slightly greater for the acetyl peptides compared with the native peptides.

*In situ* TUNEL staining showed apoptosis of lens epithelial cells in selenite-induced cataracts (Fig. 9A, panel 2, arrows), which was not observed in control lenses (Fig. 9A, panel 1). Both the native and acetyl  $\alpha A$ - and  $\alpha B$ -crystallin peptides inhibited apoptosis (Fig. 9A, panels 3–6). The activity of caspase-3 and -9 was significantly elevated in selenite-induced cataracts ( $p < 0.0005$ ), which was significantly reduced by pep-

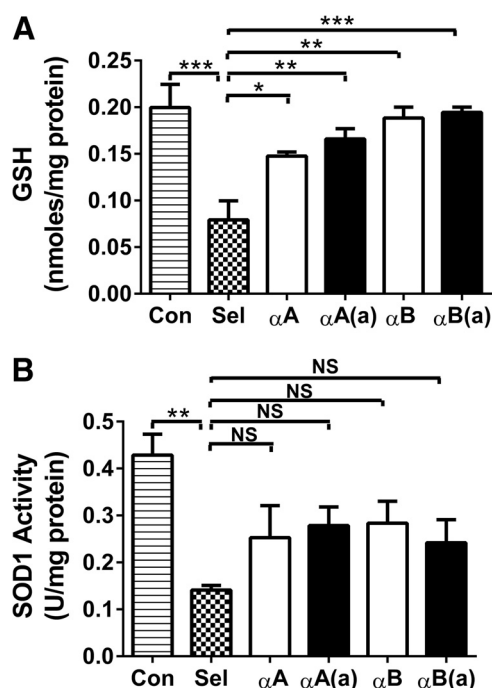


**FIGURE 8.  $\alpha$ -Crystallin peptides inhibit oxidative stress in selenite-induced cataracts.** The lenses were harvested from animals on day 6-post sodium selenite injection and processed as described under "Experimental Procedures."  $\alpha$ -Crystallin peptides (both acetyl and native peptides) administered through multiple injections of 10  $\mu$ g/animal (as in Fig. 5) inhibited the loss of GSH (panel A) and SOD1 activity in selenite-treated rat lenses (panel B). The bars represent the mean  $\pm$  S.D. of three independent experiments.  $\alpha A$ ,  $\alpha A$ -native peptide;  $\alpha A(a)$ ,  $\alpha A$ -acetyl peptide;  $\alpha B$ ,  $\alpha B$ -native peptide; and  $\alpha B(a)$ ,  $\alpha B$ -acetyl peptide. The differences between native and acetyl peptides were not statistically significant. \*,  $p < 0.05$ ; \*\*,  $p < 0.005$ ; \*\*\*,  $p < 0.0005$ . NS, not significant.

peptide treatment (except for the native  $\alpha A$ -peptide in the case of caspase-9) (Fig. 9, B and C).

The above effects were due to the translocation of the intraperitoneally injected peptide to the lens, which was verified by mass spectrometry. The low molecular weight isolate from pooled lenses from rat pups administered four injections of 100  $\mu$ g of the acetyl  $\alpha B$ -peptide was analyzed for the presence of the peptide. We detected the peptide in the lenses of peptide-injected animals (Fig. 10A). Peptides with multiple positively charged residues, such as Arg, His, and Lys, are often observed to be highly charged in ESI mass spectra. For the  $\alpha B$ -peptide, both triply and quadruply charged parent ions, 843.4560(3+) and 632.8441(4+) (Fig. 10B), were detected in the full mass spectrum (error  $< 2$  ppm). The obtained tandem mass spectra (MS/MS) confirmed the peptide sequence. As shown in Fig. 10C, the *b* series ions from *b7* through *b19* were all unmodified, which demonstrated that acetylation did not occur at Lys<sup>83</sup> or Lys<sup>90</sup>, whereas the *y2* ion observed at 288.2 (+42 Da) confirmed that Lys<sup>92</sup> is acetylated. This peptide was not detected in the control sample (Supplemental Fig. S3), even though the *m/z* values were included in the parent ion mass scan.

## DISCUSSION

The primary objective of this study was to determine whether chaperone  $\alpha$ -crystallin peptides could inhibit apoptosis in cells and experimental cataracts in animals. The second objective was to determine whether the acetyl peptides inhib-

ited apoptosis and cataracts more efficiently than the native peptides. The major findings of this work are that both  $\alpha A$ - and  $\alpha B$ -crystallin peptides are effective chaperones, and lysine acetylation has a disparate effect on the peptides: although it improves chaperone function of the  $\alpha A$ -crystallin peptide, it weakens that of the  $\alpha B$ -crystallin peptide. However, the observed surface hydrophobicity, which is thought to dictate chaperone function, was approximately identical between the acetyl and native peptides from both proteins. We cannot explain why surface hydrophobicity and chaperone function are unrelated in this case. Previous studies have reported similar findings for  $\alpha$ -crystallin (reviewed in Ref. 34). Despite these differences, the acetyl peptides were slightly better than the native peptides at inhibiting stress-induced apoptosis in cultured mammalian cells. Several findings indicate that specific inhibition of the mitochondrial apoptosis pathway was occurring: cytochrome *c* release from mitochondria and procaspase-3 activation, as well as caspase-3, caspase-9 activity were inhibited by the peptide treatment. These findings also suggest that chaperone peptides are likely to provide the sites for Bax and procaspase-3 binding and to be responsible for inhibiting cytochrome *c* release from the mitochondria by the  $\alpha$ -crystallin protein, which has been observed in previous studies (12, 16, 35, 36).

The inhibition of calcimycin-induced apoptosis observed in organ-cultured mouse lenses suggests that the peptides cross the capsule and epithelial cells in the lens. Calcimycin-induced apoptosis in lens epithelial cells occurs via the calcium-activated RAF/MEK/ERK pathway (37); therefore, we speculate that the peptides inhibit the activation of this pathway. Moreover, the inhibition of selenite-induced cataracts by the intraperitoneally injected peptides suggests that the peptides enter the circulation, cross the blood aqueous barrier, and enter the lens. The inhibition of apoptosis in these lenses further indicates that peptide function is retained after entry to the lens. The detection of the intraperitoneally injected  $\alpha B$ -crystallin peptide in the lens supports this interpretation. We found that the acetyl peptides were slightly more effective than the native peptides in these functions. This may be due to the stronger resistance of the acetyl peptides to digestion by serine proteases. Further work is necessary to clarify the mechanism underlying this phenomenon.

The prevention of cataract development by the peptides in the absence of covalent protein cross-linking in the lens (as determined by SDS-PAGE and dynamic light scattering) suggests that protein aggregation may be inhibited by blocking hydrophobic interactions and/or disulfide linkages. Previous studies have demonstrated protein degradation by proteolytic enzymes and disulfide cross-linking of proteins in selenite-induced cataracts (38, 39). It is possible that the peptides interacted directly with proteolytic enzymes and blocked their activity or bound to proteins and prevented their proteolytic degradation. Because the peptides inhibited GSH depletion and the reduction of SOD1 activity, the parallel processes of oxidative stress and protein aggregation are likely inhibited. Whether the observed inhibition of protein aggregation is directly due to peptide chaperone function or downstream effects on epithelial cells is unknown. Inhibition of epithelial cell apoptosis may

## Anti-apoptotic Properties of Crystallin Peptides

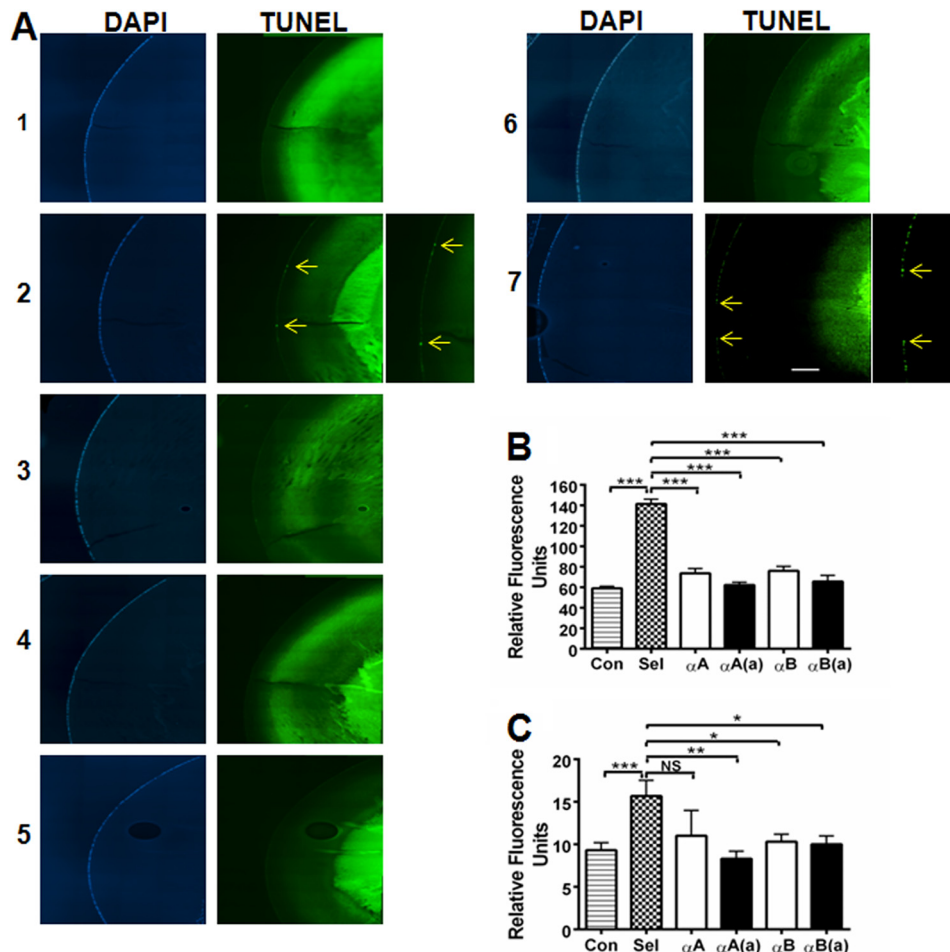


**FIGURE 9.  $\alpha$ -Crystallin peptides inhibit apoptosis through inhibition of caspases in lenses with selenite-induced cataract.** The lenses from sodium selenite- and sodium selenite + peptide-treated rat pups (multiple 10- $\mu$ g peptide injections, as in Fig. 5) were fixed and assessed for epithelial cell apoptosis using the *In situ* Cell Death Detection Kit (*panel A*). DAPI staining is shown in the *left panels*, and TUNEL staining is shown on the *right*. 1, control; *lanes 2–6*, sodium selenite treated; 2, no peptide, *arrows* indicate apoptotic cells; 3, + $\alpha$ A-native peptide; 4, + $\alpha$ A-acetyl peptide; 5, + $\alpha$ B peptide; 6, + $\alpha$ B-acetyl peptide; and 7, + $\alpha$ A scrambled peptide. The enlarged images for *panel A-2* and *A-7* are to show apoptotic cells. The elevation of caspase-3 and caspase-9 activity observed in selenite-induced cataracts was inhibited by both the native and acetyl  $\alpha$ A- and  $\alpha$ B-crystallin peptides (*panels B* and *C*). The bars represent the mean  $\pm$  S.D. of three independent experiments.  $\alpha$ A,  $\alpha$ A-native peptide;  $\alpha$ A(a),  $\alpha$ A-acetyl peptide;  $\alpha$ B,  $\alpha$ B-native peptide; and  $\alpha$ B(a),  $\alpha$ B-acetyl peptide. The intense TUNEL staining in the nuclear region is likely due to the reason stated in the legend to Fig. 4. The differences between the native and acetyl peptides were not statistically significant. \*,  $p < 0.05$ ; \*\*,  $p < 0.005$ ; \*\*\*,  $p < 0.0005$ . NS, not significant. Scale bar = 100  $\mu$ m.

be an additional mechanism that peptides use to inhibit cataract development. Furthermore, how the injected peptides were able to inhibit cataracts, when the lens already contains high levels  $\alpha$ -crystallin, is not clear. Future studies are necessary to clarify these issues.

The finding described herein that intraperitoneally injected peptides cross the blood aqueous barrier and cell plasma membrane supports the notion that these peptides exhibit important therapeutic potential, beyond inhibition of experimental cataracts. Pathogenic apoptosis is an integral component of several eye diseases, such as age-related macular degeneration, uveitis, glaucoma, and diabetic retinopathy. If the peptides can cross the blood retinal barrier, they may be useful for inhibiting apoptosis in such diseases. In fact,  $\alpha$ -crystallin delivery has been shown to reduce pericyte loss in an experimental diabetes model (40). In addition, it has been shown that  $\alpha$ A-crystallin is protective against experimentally induced autoimmune uveitis (41) and ischemic optic neuropathy (42). Furthermore, when apoptosis in

cells is accompanied by protein aggregation, such as in Alzheimer disease, the peptides may inhibit both protein aggregation and apoptosis in cells. Other potential uses of these peptides include diseases/conditions in which  $\alpha$ B-crystallin is therapeutically beneficial. Steinman and colleagues (43) elegantly demonstrated in experimental animal models that  $\alpha$ B-crystallin is effective against inflammatory neurological damage following cerebral stroke, experimentally induced autoimmune encephalomyelitis (44), multiple sclerosis (45), and cardiac ischemia-reperfusion injury (46). These peptides may be more effective than native proteins for such applications because they are smaller and may be delivered more efficiently to target tissues. Moreover, post-translational modifications that could reduce the anti-apoptotic function of  $\alpha$ -crystallin, such as Ser<sup>59</sup> phosphorylation in  $\alpha$ B-crystallin, which down-regulates its anti-apoptotic function (47), could be avoided by using peptides instead of the entire protein. Although anti-apoptotic peptide treatment may be beneficial for such conditions/diseases, caution

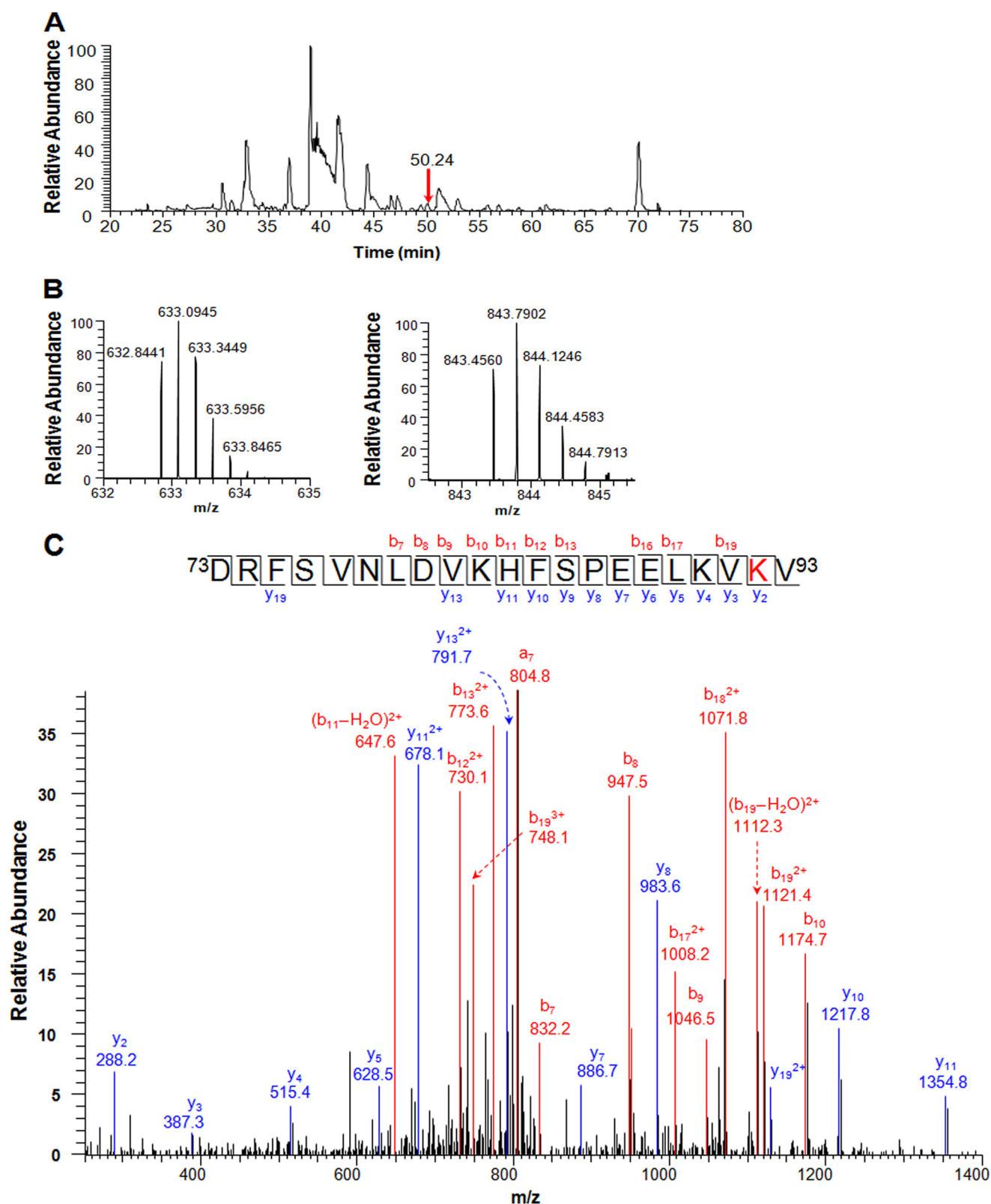


FIGURE 10. Intraperitoneally injected  $\alpha$ B-acetyl crystallin peptide translocates to the lens in rats. Rats were administered 100  $\mu$ g of the  $\alpha$ B-acetyl peptide in water intraperitoneally for 5 days. The lenses were then harvested and homogenized in 500  $\mu$ l of buffer with 6 M urea. The homogenate was filtered through a 10-kDa cut-off centrifugal filter, and the filtrate was analyzed via LC-MS/MS. Panel A shows the base peak ion chromatogram for the injected sample. The arrow indicates the peak of  $\alpha$ B-acetyl crystallin peptide. The full mass spectrum in panel B shows the triply and quadruply charged parent ions at  $m/z$  843.4560(3+) and 632.8441(4+) for the peptide. Lys<sup>92</sup> acetylation in the peptide was confirmed by MS/MS analysis of the two parent ions. The MS/MS spectrum for the triply charged ion is shown in panel C. The peptide sequence was assigned based on the fragmented  $y$ - and  $b$ -ions.

## Anti-apoptotic Properties of Crystallin Peptides

must be employed for unintended inhibition of apoptosis in off-target tissues. Hence, targeted delivery of these peptides to the appropriate tissues might be desirable for treating diseases.

*Acknowledgments*—We thank Mark Harrod for help with rat lens imaging; Catherine Doller and Dr. Scott Howell for help with histology and microscopy, Dawn Smith for help with cell culture, and Dr. Sara Tomechko of the Center for Proteomics and Bioinformatics, Case Western Reserve University, for help with the mass spectrometric data interpretation.

### REFERENCES

1. Bloemendal, H., de Jong, W., Jaenicke, R., Lubsen, N. H., Slingsby, C., and Tardieu, A. (2004) Ageing and vision. Structure, stability and function of lens crystallins. *Prog. Biophys. Mol. Biol.* **86**, 407–485
2. Andley, U. P. (2008) The lens epithelium. Focus on the expression and function of the  $\alpha$ -crystallin chaperones. *Int. J. Biochem. Cell Biol.* **40**, 317–323
3. Horwitz, J. (1992)  $\alpha$ -Crystallin can function as a molecular chaperone. *Proc. Natl. Acad. Sci. U.S.A.* **89**, 10449–10453
4. Srinivasan, A. N., Nagineni, C. N., and Bhat, S. P. (1992)  $\alpha$ A-Crystallin is expressed in non-ocular tissues. *J. Biol. Chem.* **267**, 23337–23341
5. Dubin, R. A., Wawrousek, E. F., and Piatigorsky, J. (1989) Expression of the murine  $\alpha$ B-crystallin gene is not restricted to the lens. *Mol. Cell Biol.* **9**, 1083–1091
6. Horwitz, J. (2003)  $\alpha$ -Crystallin. *Exp. Eye Res.* **76**, 145–153
7. Zhang, Z. F., Zhang, J., Hui, Y. N., Zheng, M. H., Liu, X. P., Kador, P. F., Wang, Y. S., Yao, L. B., and Zhou, J. (2011) Up-regulation of NDRG2 in senescent lens epithelial cells contributes to age-related cataract in human. *PLoS One* **6**, e26102
8. Yan, Q., Liu, J. P., and Li, D. W. (2006) Apoptosis in lens development and pathology. *Differentiation* **74**, 195–211
9. Aoyama, A., Fröhli, E., Schäfer, R., and Klemenz, R. (1993)  $\alpha$ B-Crystallin expression in mouse NIH 3T3 fibroblasts. Glucocorticoid responsiveness and involvement in thermal protection. *Mol. Cell Biol.* **13**, 1824–1835
10. Dasgupta, S., Hohman, T. C., and Carper, D. (1992) Hypertonic stress induces  $\alpha$ B-crystallin expression. *Exp. Eye Res.* **54**, 461–470
11. Mehlen, P., Preville, X., Chareyron, P., Briolay, J., Klemenz, R., and Arrigo, A. P. (1995) Constitutive expression of human hsp27, *Drosophila* hsp27, or human  $\alpha$ B-crystallin confers resistance to TNF- and oxidative stress-induced cytotoxicity in stably transfected murine L929 fibroblasts. *J. Immunol.* **154**, 363–374
12. Pasupuleti, N., Matsuyama, S., Voss, O., Doseff, A. I., Song, K., Danielpour, D., and Nagaraj, R. H. (2010) The anti-apoptotic function of human  $\alpha$ A-crystallin is directly related to its chaperone activity. *Cell Death Dis.* **1**, e31
13. Andley, U. P., Song, Z., Wawrousek, E. F., Fleming, T. P., and Bassnett, S. (2000) Differential protective activity of  $\alpha$ A- and  $\alpha$ B-crystallin in lens epithelial cells. *J. Biol. Chem.* **275**, 36823–36831
14. Andley, U. P. (2007) Crystallins in the eye. Function and pathology. *Prog. Retin Eye Res.* **26**, 78–98
15. Andley, U. P. (2009) Effects of  $\alpha$ -crystallin on lens cell function and cataract pathology. *Curr. Mol. Med.* **9**, 887–892
16. Mao, Y. W., Liu, J. P., Xiang, H., and Li, D. W. (2004) Human  $\alpha$ A- and  $\alpha$ B-crystallins bind to Bax and Bcl-X(S) to sequester their translocation during staurosporine-induced apoptosis. *Cell Death Differ.* **11**, 512–526
17. Liu, J. P., Schlosser, R., Ma, W. Y., Dong, Z., Feng, H., Lui, L., Huang, X. Q., Liu, Y., and Li, D. W. (2004) Human  $\alpha$ A- and  $\alpha$ B-crystallins prevent UVAQ-induced apoptosis through regulation of PKC $\alpha$ , RAF/MEK/ERK and AKT signaling pathways. *Exp. Eye Res.* **79**, 393–403
18. Kannan, R., Sreekumar, P. G., and Hinton, D. R. (2012) Novel roles for  $\alpha$ -crystallins in retinal function and disease. *Prog. Retin. Eye Res.* **31**, 576–604
19. Masilamoni, J. G., Jesudason, E. P., Bharathi, S. N., and Jayakumar, R. (2005) The protective effect of  $\alpha$ -crystallin against acute inflammation in mice. *Biochim. Biophys. Acta* **1740**, 411–420
20. Harrington, V., Srivastava, O. P., and Kirk, M. (2007) Proteomic analysis of water insoluble proteins from normal and cataractous human lenses. *Mol. Vis.* **13**, 1680–1694
21. Wilmarth, P. A., Tanner, S., Dasari, S., Nagalla, S. R., Riviere, M. A., Bafna, V., Pevzner, P. A., and David, L. L. (2006) Age-related changes in human crystallins determined from comparative analysis of post-translational modifications in young and aged lens. Does deamidation contribute to crystallin insolubility? *J. Proteome Res.* **5**, 2554–2566
22. Hains, P. G., and Truscott, R. J. (2007) Post-translational modifications in the nuclear region of young, aged, and cataract human lenses. *J. Proteome Res.* **6**, 3935–3943
23. Nagaraj, R. H., Sell, D. R., Prabhakaram, M., Ortwerth, B. J., and Monnier, V. M. (1991) High correlation between pentosidine protein cross-links and pigmentation implicates ascorbate oxidation in human lens senescence and cataractogenesis. *Proc. Natl. Acad. Sci. U.S.A.* **88**, 10257–10261
24. Nagaraj, R. H., Nahomi, R. B., Shanthakumar, S., Linetsky, M., Padmanabha, S., Pasupuleti, N., Wang, B., Santhoshkumar, P., Panda, A. K., and Biswas, A. (2012) Acetylation of  $\alpha$ A-crystallin in the human lens. Effects on structure and chaperone function. *Biochim. Biophys. Acta* **1822**, 120–129
25. Sharma, K. K., Kumar, R. S., Kumar, G. S., and Quinn, P. T. (2000) Synthesis and characterization of a peptide identified as a functional element in  $\alpha$ A-crystallin. *J. Biol. Chem.* **275**, 3767–3771
26. Bhattacharyya, J., Padmanabha Udupa, E. G., Wang, J., and Sharma, K. K. (2006) Mini- $\alpha$ B-crystallin. A functional element of  $\alpha$ B-crystallin with chaperone-like activity. *Biochemistry* **45**, 3069–3076
27. Staniszevska, M. M., and Nagaraj, R. H. (2006) Up-regulation of glyoxalase I fails to normalize methylglyoxal levels. A possible mechanism for biochemical changes in diabetic mouse lenses. *Mol. Cell Biochem.* **288**, 29–36
28. Voss, O. H., Batra, S., Kolattukudy, S. J., Gonzalez-Mejia, M. E., Smith, J. B., and Doseff, A. I. (2007) Binding of caspase-3 prodomain to heat shock protein 27 regulates monocyte apoptosis by inhibiting caspase-3 proteolytic activation. *J. Biol. Chem.* **282**, 25088–25099
29. Padival, S., and Nagaraj, R. H. (2006) Pyridoxamine inhibits maillard reactions in diabetic rat lenses. *Ophthalmic Res.* **38**, 294–302
30. Kakkar, P., Das, B., and Viswanathan, P. N. (1984) A modified spectrophotometric assay of superoxide dismutase. *Indian J. Biochem. Biophys.* **21**, 130–132
31. Santhoshkumar, P., and Sharma, K. K. (2006) Conserved F84 and P86 residues in  $\alpha$ B-crystallin are essential to effectively prevent the aggregation of substrate proteins. *Protein Sci.* **15**, 2488–2498
32. Li, W. C., Kuszak, J. R., Wang, G. M., Wu, Z. Q., and Spector, A. (1995) Calcimycin-induced lens epithelial cell apoptosis contributes to cataract formation. *Exp. Eye Res.* **61**, 91–98
33. Shearer, T. R., Ma, H., Fukiage, C., and Azuma, M. (1997) Selenite nuclear cataract. Review of the model. *Mol. Vis.* **3**, 8
34. Reddy, G. B., Kumar, P. A., and Kumar, M. S. (2006) Chaperone-like activity and hydrophobicity of  $\alpha$ -crystallin. *IUBMB Life* **58**, 632–641
35. Kamradt, M. C., Chen, F., and Cryns, V. L. (2001) The small heat shock protein  $\alpha$ B-crystallin negatively regulates cytochrome *c*- and caspase-8-dependent activation of caspase-3 by inhibiting its autoproteolytic maturation. *J. Biol. Chem.* **276**, 16059–16063
36. Ghosh, J. G., Shenoy, A. K., Jr., and Clark, J. I. (2007) Interactions between important regulatory proteins and human  $\alpha$ B-crystallin. *Biochemistry* **46**, 6308–6317
37. Li, D. W., Liu, J. P., Mao, Y. W., Xiang, H., Wang, J., Ma, W. Y., Dong, Z., Pike, H. M., Brown, R. E., and Reed, J. C. (2005) Calcium-activated RAF/MEK/ERK signaling pathway mediates p53-dependent apoptosis and is abrogated by  $\alpha$ B-crystallin through inhibition of RAS activation. *Mol. Biol. Cell* **16**, 4437–4453
38. David, L. L., and Shearer, T. R. (1984) State of sulfhydryl in selenite cataract. *Toxicol. Appl. Pharmacol.* **74**, 109–115
39. David, L. L., and Shearer, T. R. (1984) Calcium-activated proteolysis in the lens nucleus during selenite cataractogenesis. *Invest. Ophthalmol. Vis. Sci.* **25**, 1275–1283
40. Kim, Y. H., Park, S. Y., Park, J., Kim, Y. S., Hwang, E. M., Park, J. Y., Roh,

- G. S., Kim, H. J., Kang, S. S., Cho, G. J., and Choi, W. S. (2012) Reduction of experimental diabetic vascular leakage and pericyte apoptosis in mice by delivery of  $\alpha$ A-crystallin with a recombinant adenovirus. *Diabetologia* **55**, 2835–2844
41. Rao, N. A., Saraswathy, S., Pararajasegaram, G., and Bhat, S. P. (2012) Small heat shock protein  $\alpha$ A-crystallin prevents photoreceptor degeneration in experimental autoimmune uveitis. *PLoS One* **7**, e33582
42. Pangratz-Fuehrer, S., Kaur, K., Ousman, S. S., Steinman, L., and Liao, Y. J. (2011) Functional rescue of experimental ischemic optic neuropathy with  $\alpha$ B-crystallin. *Eye (Lond.)* **25**, 809–817
43. Arac, A., Brownell, S. E., Rothbard, J. B., Chen, C., Ko, R. M., Pereira, M. P., Albers, G. W., Steinman, L., and Steinberg, G. K. (2011) Systemic augmentation of  $\alpha$ B-crystallin provides therapeutic benefit 12 hours post-stroke onset via immune modulation. *Proc. Natl. Acad. Sci. U.S.A.* **108**, 13287–13292
44. Kurnellas, M. P., Brownell, S. E., Su, L., Malkovskiy, A. V., Rajadas, J., Dolganov, G., Chopra, S., Schoolnik, G. K., Sobel, R. A., Webster, J., Ousman, S. S., Becker, R. A., Steinman, L., and Rothbard, J. B. (2012) Chaperone activity of small heat shock proteins underlies therapeutic efficacy in experimental autoimmune encephalomyelitis. *J. Biol. Chem.* **287**, 36423–36434
45. Ousman, S. S., Tomooka, B. H., van Noort, J. M., Wawrousek, E. F., O'Connor, K. C., Hafler, D. A., Sobel, R. A., Robinson, W. H., and Steinman, L. (2007) Protective and therapeutic role for  $\alpha$ B-crystallin in autoimmune demyelination. *Nature* **448**, 474–479
46. Velotta, J. B., Kimura, N., Chang, S. H., Chung, J., Itoh, S., Rothbard, J., Yang, P. C., Steinman, L., Robbins, R. C., and Fischbein, M. P. (2011)  $\alpha$ B-crystallin improves murine cardiac function and attenuates apoptosis in human endothelial cells exposed to ischemia-reperfusion. *Ann. Thorac. Surg.* **91**, 1907–1913
47. Launay, N., Tarze, A., Vicart, P., and Lilienbaum, A. (2010) Serine 59 phosphorylation of  $\alpha$ B-crystallin down-regulates its anti-apoptotic function by binding and sequestering Bcl-2 in breast cancer cells. *J. Biol. Chem.* **285**, 37324–37332